

4.11 NOCTURNAL LOW-LEVEL JET CHARACTERISTICS OVER SOUTHERN COLORADO

Yelena L. Pichugina^{*1}, R. M. Banta², N. D. Kelley³, S. P. Sandberg², J. L. Machol⁴, and W. A. Brewer²

¹Science and Technology Corporation, Boulder, CO

²Environmental Technology Laboratory (ETL), NOAA, Boulder, CO

³National Renewable Energy Laboratory, Golden, CO

⁴CIRES, University of Colorado and NOAA ETL, Boulder, CO

1. INTRODUCTION

An intensive field-measurement campaign designed to characterize mean and turbulent Low Level Jet (LLJ) properties was carried out at a site to the south of Lamar, Colorado 1-16 September 2003. The site was chosen as a planned wind farm development site. The instrumentation involved in this campaign included the High Resolution Doppler Lidar (HRDL) deployed by the Environmental Technology Laboratory (ETL) of the National Oceanic and Atmospheric Administration (NOAA), a 120-m tall meteorological tower installed by General Electric Wind Energy (GE Wind) and an acoustic wind profiler or Doppler sodar installed by the National Renewable Energy Laboratory (NREL).

2. OBJECTIVES.

The main objectives of this study include the following:

- To determine the usefulness of HRDL for wind-energy resource assessment at heights up to 200 m above ground level.
- To investigate nighttime behavior of LLJ and LLJ characteristics.
- To contrast low-level jet properties with those observed during the CASES-99 campaign, which took place in eastern Kansas in October 1999.

3. INSTRUMENT LOCATIONS

The geographical coordinates of the tower

** Corresponding author address:*
Yelena L. Pichugina, ETL / NOAA, 325
Broadway, Boulder, CO 80305;
e-mail: Yelena.Pichugina@noaa.gov

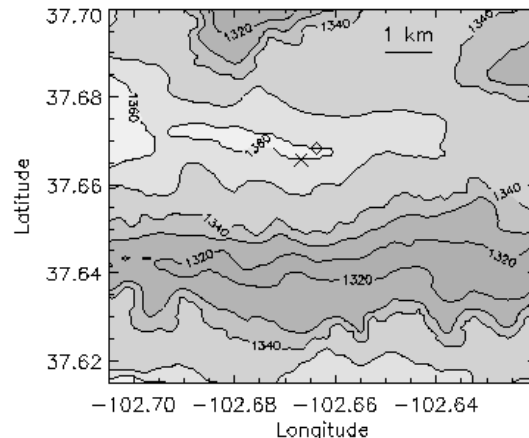


Figure 1. Map of the study area near Lamar, CO showing the locations of HRDL (x) and tower (◇).

were 37.6683° N and 102.66375° W. Its base was at an elevation of 1357 m above mean sea level. The tower instruments included three-axis sonic anemometers mounted at heights of 54, 67, 85, and 116 m to provide three-component wind and temperature data at a sampling rate of 20 Hz. The sodar was located 109 m to the southeast of the tower base. This location was chosen to be as close as possible to the tower to obtain a better comparison of profiler derived winds with those directly measured by instruments on the tower. Both tower instruments and sodar were in operation for two summers prior to the campaign as described by Kelley et al. (2004). HRDL was located at the same elevation as the tower and sodar with coordinates 37.6657° N and 102.6668° W. It provided information about mean LLJ characteristics (speed, height, and direction) as well as both vertical and horizontal details of organized turbulent structures found beneath these jets at altitudes now occupied by the 70-m diameter wind rotors of the 108 General Electric 1.5 MW wind turbines at the Colorado Green Wind Farm. HRDL was described by Grund et al. (2001), Wulfmeyer et al. (2000), and Banta et

al. (2002). Figure 1 shows the location of the instrumentation at the site.

4. HIGH-RESOLUTION DOPPLER LIDAR DATA

Approximately 120 hours of HRDL data were collected at night time from local sunset (0:00 UTC) until sunrise (10:00-11:00 UTC). Data sets for eleven entire nights were obtained. Additional data sets on 1, 4, 7 and 8 September were incomplete due to technical problems or weather conditions.

During periods of operation, HRDL performed a variety of different scans to address different scanning objectives. It was typical to start each hour of observations with short sequence conical or plan position indicator (PPI) scans. These scans are performed by varying the azimuth angle of the lidar beam in the full range 0-360° at a fixed elevation angle. After several minutes of conical scans, vertical-slice scans, also called range-height indicator (RHI) scans, were typically performed for 30-40 min. These scans are performed by varying the elevation angle of the lidar beam with fixed azimuth angle. Vertical-slice scans were generally performed looking approximately along the mean wind vector estimated from conical scans. During the night several stare scans, where the lidar beam pointed in one direction, were performed. These staring scans are not used in this paper.

To retrieve a regular sampling of vertical wind profiles from the lidar data set, we used an algorithm developed to analyze the CASES-99 data set that involves a modification to the conventional velocity-azimuth display (VAD) processing technique (Browning and Wexler 1968). This procedure is described by Banta et al. (2002) and Chai et al. (2003).

The CASES-99 (Cooperative Surface-Atmosphere Exchange study) field program, carried out in the Great Plains during October 1999, was described by Blumen et al (2001) and Poulos et al (2002). Characteristics and evolution of the LLJ over southeastern Kansas, the operating characteristics of HRDL and a detailed description of data processing techniques for both conical and vertical-slice scans described by Banta et al. (2002) and Newsom and Banta (2002).

5. RESULTS

The processing techniques just described were applied to the entire Lamar data set using 1-, 10-, or 15-min averaging periods. Profiles of the mean velocity component U parallel to the scan plane and its variance U_{VAR} were computed from vertical-slice scans for each of the eleven nights when HRDL had good data. An example of a time-height cross section of mean wind and wind-speed variance for the night of 15 September is given in Figure 2.

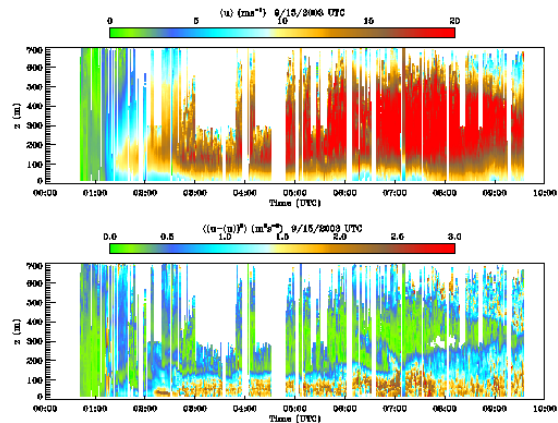


Figure 2. Sample time-height cross sections of mean wind speed (top panel) and variance of the radial wind component (bottom panel) calculated from HRDL vertical-slice scans during night of September 15. Each vertical line represents a vertical profile of the horizontally averaged wind speed or variance from the vertical cross sections. Horizontal velocity profiles were derived from individual vertical-slice scans by sorting the data into 10-m vertical bins. Estimates of the mean and variance were then obtained for each bin.

Wind speed measured by sonic anemometers at four tower levels were compared with mean winds derived from vertical-slice scans and averaged in 10-m vertical bins close to these levels. Figure 3 represents an example of wind speed and mean wind time series for the night of 5 September. Slight differences in wind speed data derived from both instruments can be explained by the difference in the temporal and spatial averaging of sonic and HRDL data.

6. LOW-LEVEL JET

The nocturnal LLJ has a role in generating shear and turbulence between the level of maximum wind speed Z_X and the earth's surface, and thus can strongly influence surface-atmosphere exchange at night.

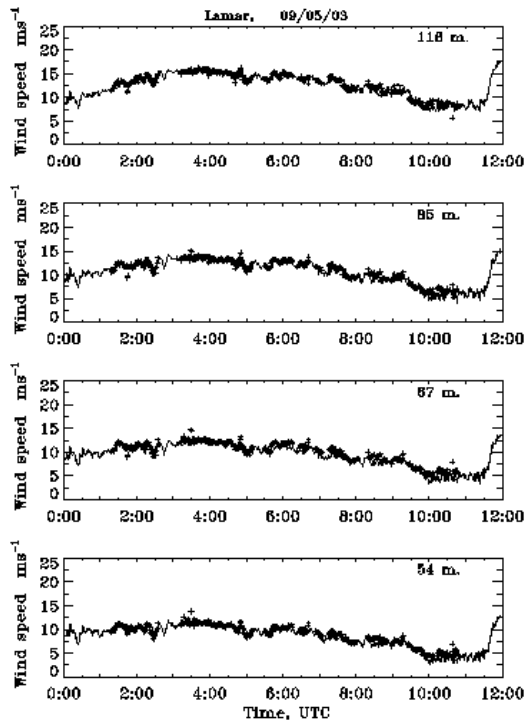


Figure 3. Time series of wind speed (solid line) from sonic anemometer data at the tower levels 116, 85, 67 and 54 m (top to bottom) and the horizontal wind component (+) calculated from HRDL vertical-slice scans and averaged in 10-m vertical bins.

Profiles taken by HRDL were available at time intervals of < 1 min with vertical resolutions of < 10 m for the entire set of nights, allowing the evolution of the nocturnal LLJ to be described in detail. Important aspects of the LLJ were its spatial variability and temporal evolution. On most HRDL vertical-slice scans, the jet was horizontal across the 2 to 3 km expanse of the scan, but at times the height varied significantly over the scan, often apparently following the local terrain. The jet generally formed over a 3-h transition period after sunset, with the jet speed often reaching several temporal maxima at 3-5 h intervals through the night. The sequence of vertical-slice scans for the night of September 15 is given in Figure 4 to illustrate LLJ formation. As shown in Figure 4 a disorganized jet started to form at 100 m AGL and in less than 30 min (by 1:51 UTC) the jet formed an organized layer at ~ 130 m. The objective criteria we used to define a LLJ were based on those of Andreas et al. (2000), with a slight modification for choosing those low-level wind-speed maxima that exhibited a decrease of at

least 0.5 m s^{-1} at vertical levels both above and below the level of the peak.

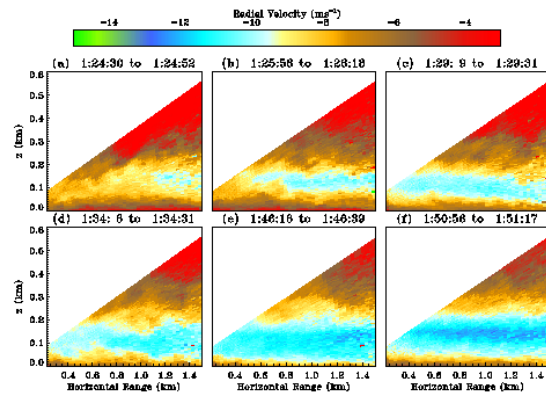


Figure 4. RHI scans of radial velocity on 15 September show a rapid nighttime LLJ formation two hours after local sunset (0:00 UTC).

To investigate finer details of the LLJ nighttime behavior we analyzed the series of LLJ characteristics U_x and Z_x through the night (Figure 5). This analysis is based on 1-min averaged data. Following Banta et al. (2002), the nights have been divided into four categories: high wind ($15\text{-}20 \text{ m s}^{-1}$), high-moderate winds ($10\text{-}15 \text{ m s}^{-1}$), low-moderate wind ($5\text{-}10 \text{ m s}^{-1}$), and low-wind ($0\text{-}5 \text{ m s}^{-1}$). The distributions of the wind speed maxima in four categories are given in Table 1.

As shown in the table, most of the nights (5, 6, 9, 10 and 15) fell into the high wind category.

Day	Low $0 < U_x < 5$	Low-moderate $5 < U < 10$	High-moderate $10 < U_x < 15$	High $U_x > 15$
02	0	96.5	3.5	0
03	0	33.6	66.4	0
05	0	3.7	20.6	75.7
06	0	0	14.6	85.4
09	8.3	11.4	8.4	71.9
10	0	4.3	0.9	94.8
11	0	4.2	69.5	26.3
12	13.7	84.6	1.7	0
13	0	16.7	52.3	31.0
15	2.7	3.9	14.4	79.0
16	5.4	63.6	28.3	2.7

Table 1. Distributions (in percent) of the wind speed maximum by four categories: high wind ($15\text{-}20 \text{ m s}^{-1}$), high-moderate wind ($10\text{-}15 \text{ m s}^{-1}$), low-moderate wind ($5\text{-}10 \text{ m s}^{-1}$), and low-wind ($0\text{-}5 \text{ m s}^{-1}$).

The rest of the nights were divided between the high-moderate (3, 11 and 13) and the low-moderate (2, 12 and 16) wind-speed categories. Time series of LLJ characteristics determined from HRDL vertical-slice scans for a high (a), a moderate (b) and a low-moderate (c) wind speed night are given in Figure 5.

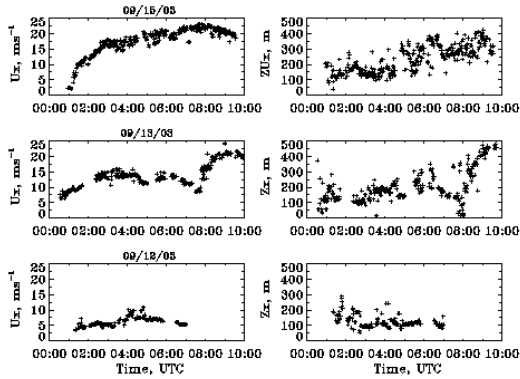


Figure 5. Time-series plots of nighttime LLJ characteristics determined from HRDL vertical-slice scans for high-jet-speed ($>15 \text{ m s}^{-1}$) (top panel), high-moderate jet speed ($10\text{--}15 \text{ m s}^{-1}$) and low-moderate jet speed ($<10 \text{ m s}^{-1}$) (bottom). The ordinate of the left column is the maximum jet speed U_x (m s^{-1}). The right column ordinate is the height of maximum speed Z_x .

Nights when U_x was greater than 15 m s^{-1} exhibited very similar LLJ speed behavior. The jet formed during the first two hours after local sunset (0:00–2:00 UTC) and then fluctuated around its maximum (20 to 25 m s^{-1}) over the next four to six hours. In early morning hours (8:00–10:00 UTC) U_x decreased but remained greater than 15 m s^{-1} . Z_x varied in time between 200 and 400 m . In the high-moderate wind speed nights ($10\text{--}15 \text{ m s}^{-1}$) the jet reached its maximum several times during the night, showing minimum speeds in the early morning hours. Z_x was again much more variable both in time and in space than U_x and varied between 100 and 400 m . As with the CASES-99 data the variability in Z_x was often due to ambiguities in its determination from profile data.

Both of the low-moderate nights with complete data sets (12 and 16 September) started out with a low, weak jet, which reached its maximum by 04:00 UTC and then decreased in the morning. Z_x was much lower than in previous categories and varied between $50\text{--}200 \text{ m}$. Only a few hours of HRDL data (4:00–8:00 UTC) were recorded on 2

September. During this period U_x and Z_x were remarkably steady with light variations around 10 m s^{-1} and 80 m respectively. Analysis of the wind-speed time series derived from the sonic data provides confidence in referring to this entire night as a low-moderate.

As an extension of the time series analysis, we also investigated the gradient Richardson number (Ri) calculated from 1-min averaged sonic anemometer data at the tower levels 54 and 116 m for all nights in each wind speed category. This analysis indicated that the highest wind speeds were associated with the smallest Ri, as expected. The condition $\text{Ri} < 0.25$ was true for all high-speed nights. For the high-moderate nights the maximum of the Ri histogram was located just to the right of critical range (>0.25). For the low-moderate nights, Ri was distributed over values of $0.25\text{--}2$ with a peak at ~ 1 . As an example, the Ri distributions for the high speed (09/15), the high-moderate (09/13) and the low-moderate nights are given in Figure 6.

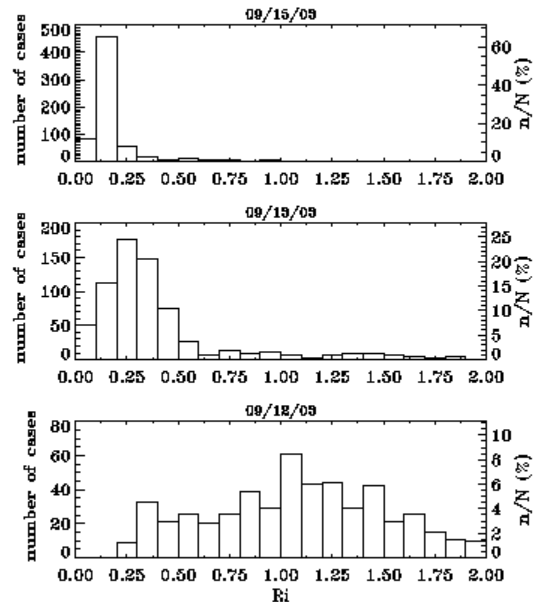


Figure 6. Distribution of gradient Richardson number (Ri) calculated from 1-min averaged sonic anemometer data during the high (09/15), the high-moderate (09/13) and the low-moderate (09/12) speed nights.

The distributions of the frequency of occurrence of LLJ characteristics based on HRDL 15-min means of U_x and Z_x (Figure 7) were compared to results obtained during the CASES-99 experiment as described in Banta et al (2002). The speeds of the jet maxima spread between 5 and 20 m s^{-1} with the biggest modes $17\text{--}18$, $14\text{--}15$ and $9\text{--}10 \text{ m}$

s^{-1} , as compared with only one clear mode at 8-9 $m s^{-1}$ in the CASES-99 data. The height of the LLJ fell into the 90-200 m range with the two biggest modes at 180-190 and 100-110 m, whereas in CASES-99 the single mode was just below 100 m. The mode of nearly 6% of the occurrences at 300 m is consistent with the results of US Great Plains studies (Whiteman et al. 1997).

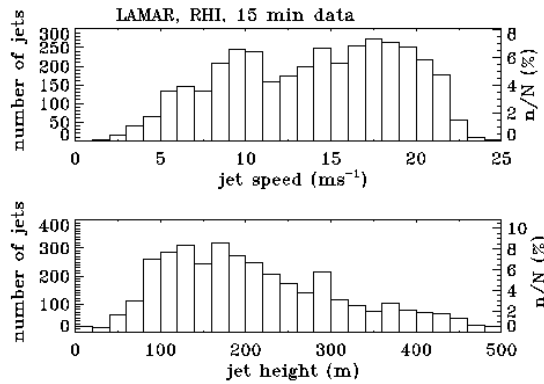


Figure 7 Histograms of jet speed U_x (top panel) and height Z_x of maximum speed (bottom) for 1-min averages. Percentages of occurrences in each bin are shown along left vertical axis, and total number of occurrences in each bin is indicated along the right vertical axis.

As an extension of the histogram analysis, a scatter diagram of Z_x versus U_x , is presented in Figure 8. Similar to the CASES-99 plot of Z_x versus U_x , this plot shows a tendency for the stronger LLJs to occur at higher altitudes than the weaker ones with a correlation coefficient of 0.71. As shown in Figure 8, jets with speed maxima above 10 $m s^{-1}$ that occurred at very low levels could be potentially damaging to wind turbines.

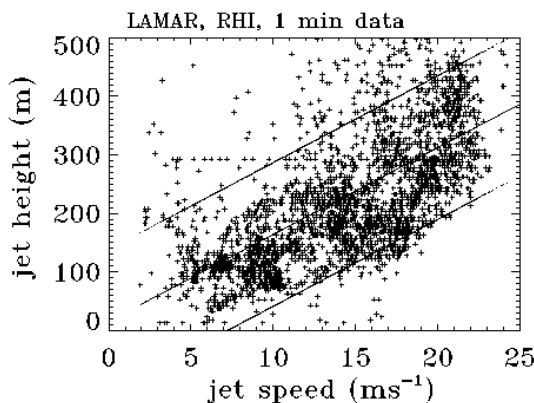


Figure 8 Scatter diagrams of Z_x vs U_x . Data were compiled from 1-min means of each quantity determined from HRDL vertical-slice scans. The middle line

represents the best-fit linear regression ($R=0.71$) and the upper and lower lines are for ± 1 standard deviation.

7. CONCLUSIONS

The fine resolution of the HRDL data has allowed us to focus on the first wind speed maximum above the surface produced by nocturnal decoupling of the flow, for comparison with similar analyses of the CASES-99 data. This maximum is most likely responsible for the production of shear and the generation of turbulence between the surface and the LLJ. Understanding its behavior is believed to be critical to further understanding of nighttime mixing processes between the atmosphere and the surface. Some overall objectives of the present study were to determine the typical characteristics (height Z_x and speed U_x) of the LLJ's seen during the Lamar 2003 experiment, to investigate the spatial variability of the LLJ characteristics, and to study the evolution of the LLJ characteristics through eleven nights.

The Lamar experiment took place in the High Plains of eastern Colorado during September when summer conditions still prevailed. This allowed the opportunity to contrast Lamar low-level jet properties with those observed during CASES-99, which took place in eastern Kansas in October. Comparison of Lamar and CASES-99 results shows that the LLJ maxima tended to be higher and stronger during Lamar than for CASES-99.

The biggest mode in the U_x , histogram was at 17-18 $m s^{-1}$, and the biggest mode in Z_x was at 160-170 m, whereas for CASES-99 these modes were at 8 $m s^{-1}$ and 90 m respectively. The high frequency (about 18%) of jets at Lamar with Z_x between 50 and 120 m AGL is potentially significant for wind-energy applications. The CASES-99 time series of jet characteristics showed that, except for the strongest wind cases, U_x , tended to be relatively constant, whereas Z_x was much more variable. This suggests that changes in the shear below the jet could be due to changes in the height rather than the speed of the jet.

These findings are important to wind energy applications and to a complete understanding of stable boundary layer processes, including evaluation of the effects of near surface fluxes in the vertical distribution of quantities through a nighttime period.

Acknowledgments. Field data acquisition and much of the analysis for this research was funded by the National Renewable Energy Research Laboratory (NREL) of the U.S. Department of Energy (DOE) under Interagency Agreement DOE-AI36-03GO13094. Portions of the analysis were also supported by the U.S. Army Research Office (Dr. Walter Bach) of the Army Research Laboratory under Proposal No. 43711-EV. We thank our colleagues Brandi McCarty, Joanne George, Lisa Darby, Andreas Muschinski, Jennifer Keane, Ann Weickmann, Ron Richter, and Raul Alvarez from ETL, and the following from NREL: Mari Shirazi, Dave Jager, S. Wilde and J. Adams. We also wish to acknowledge the Emick family, on whose ranch this project took place.

REFERENCES

- Andreas, E. L., K. J. Claffey, and A. P. Makshtas, 2000: Low-Level Atmospheric Jets and Inversion over the Western Weddel Sea, *Boundary-Layer Meteorol.* **97**, 459-486.
- Banta, R.M., R.K. Newsom, J.K. Lundquist, Y.L. Pichugina, R.L. Coulter, and L. Mahrt, 2002: Nocturnal low-level jet characteristics over Kansas during CASES-99. *Boundary-Layer Meteorol.*, **105**, 221-252.
- Blumen, W., R.M. Banta, S.P. Burns, D.C. Fritts, R. Newsom, G.S. Poulos, and J. Sun, 2001: Turbulence statistics of a Kelvin-Helmholtz billow event observed in the nighttime boundary layer during the CASES-99 field program. *Dynamics of Atmos. and Oceans*, **34**, 189-204.
- Chai, T., C. L. Lin, R. K Newsom, 2003: Retrieval of microscale flow structure from high resolution Doppler lidar using an adjoint model. *J. Atmos. Sci.*, accepted.
- Grund, C. J., R. M. Banta, J. L. George, J. N. Howell, M. J. Post, R. A. Richter, A. M. Weickmann, 2001: High-resolution Doppler lidar for boundary layer and cloud research. *J. Atmos. Oceanic Technol.*, **18**, 376-393.
- Kelley, N, M. Shirazi, D. Jager, S. Wilde, J. Adams, M. Buhl, P. Sullivan, and E. Patton, 2004. Lamar Low-Level Jet Project Interim Report. National Renewable Energy Laboratory Technical Report.
- Newsom, R.K., and R.M. Banta, 2003: Shear-flow instability in the stable nocturnal boundary layer as observed by Doppler lidar during CASES-99. *J. Atmos. Sci.*, **30**, 16-33.
- Poulos, G.S., W. Blumen, D.C. Fritts, J.K. Lundquist, J. Sun, S. Burns, C. Nappo, R.M. Banta, R.K. Newsom, J. Cuxart, E. Terradellas, B. Balsley, M. Jensen, 2002: CASES-99: A comprehensive investigation of the stable nocturnal boundary layer. *Bull. Amer. Meteorol. Soc.*, **83**, 555-581.
- Whiteman, C. D., X. Bian, and S. Zhong, 1997: Low-Level Jet Climatology from Enhanced Rawinsonde Observations at a Site in the Southern Great Plains, *J. Appl. Meteorol.* **36**, 1363-1367.
- Wulfmeyer, V.O., Randall, M., Brewer, W. A., and Hardesty R. M., 2000: 2 μ m Doppler Lidar Transmitter with High Frequency Stability and Low Chirp, *Opt. Lett.* **25**, 1228-1230.